Proceedings of the
International Conference on Mechanical Engineering and Renewable Energy 2013
(ICMERE2013) 1 – 3 May 2014, Chittagong, Bangladesh

ICMERE2013-PI-109

A SINGLE AIR BUBBLE RISE IN WATER: A CFD STUDY

Md. Tariqul Islam[1*], P. Ganesan[2], J. N. Sahu[3], Md. Nasir Uddin[4] and Abdul mannan[5]

[1, 2]Department of Mechanical, Faculty of Engineering, University of Malaya, 50603, Kuala Lumpur, Malaysia
[3,4]Department of Chemical, Faculty of Engineering, University of Malaya, 50603, Kuala Lumpur, Malaysia
[5]Atish Dipankar University of Science & Technology, Dhaka, Bangladesh

[1,*]oly_05me@yahoo.com

Abstract*-In this paper, the combined level set (LS) and volume of fluid (VOF) method has been used to numerically investigate the rising behaviour of a single gas bubble through the stagnant liquid in a rectangular domain and trapezoidal domain using Fluent on Computation fluid dynamics (CFD) platform. A single air bubble rises into stagnant water has been considered and modelled for three different bubble sizes. A set of transient conversion equations of continuity, momentum, surface tension and gravitational force effects were solved by pressure implicit splitting operator (PISO) algorithm and a piecewise linear interface calculation (PLIC) was applied to solve the movement of gas-liquid interface characteristic. The simulation result of air bubble rise behaviour was well agreement with available literature results. It is found that the bubble rise behaviour was different in different shape of column, such as: bubble rising distance, terminal velocity and bubble flow field.*

Keywords: Computation fluid dynamics (CFD), Volume of fluid (VOF), Terminal velocity.

1. INTRODUCTION

Gas–liquid bubble columns are commonly used as multiphase reactors in chemical, biochemical and industrial process, etc., for its advantages such as a high mass and heat transfer and an effective inter-phase contact [1-4]. In bubble column, the motion of bubbles can be very complex due to high density and viscosity ratios. It is also difficult to obtain an accurate mathematical model that can be used to calculate the bubble rise velocity in various physical properties and system parameters. The bubble rise behaviours are strongly depends on a bubble size and gas-liquid properties likes density, viscosity and surface tension [2]. Therefore, it is important to understand the basic knowledge of the complex bubble flow. In recent year, computational fluid dynamics (CFD) with the enhancement of numerical algorithms and computing power, a better physical understanding of two-phase flow problem likes a single bubble rising behaviour can be obtained.

The volume of fluid (VOF) method in the Ansys-Fluent CFD commercial package [20] has been used for simulation of the two-phase flow. VOF is a well-known technique for an interface tracking of the motion of all phases, which is included in the governing equation and continuum surface force (CSF) equation at the interface[5-10]. In addition, the level-set (LS) method [6, 11, 12] is used with VOF to improve the interface tracking and bubble shapes in the current study.

The purpose of this study is to carry out numerical investigations of gas bubbles of different sizes rising in water in different shapes of column.

2. METHODOLOGY

For incompressible flow and a constant density fluid, the continuity and momentum equations are as follows-

$$\nabla.\mathbf{u} = 0 \tag{1}$$

$$\frac{\partial(\rho\mathbf{u})}{\partial t} + \nabla.(\rho\mathbf{u}\mathbf{u}) = -\nabla p + \nabla.\tau + \rho\mathbf{g} + \mathbf{F_b} \tag{2}$$

$$\tau = [\mu\{\nabla\mathbf{u} + (\nabla\mathbf{u})^T\}]$$

where $\mathbf{u}$ is the velocity vector,$\rho$is the density and $\mu$is the viscosity, p is the pressure, g= $(0, -g)$ is the gravitational acceleration and τ is stress tensor.

The dynamic stress balance is realized through the CSF model, which is incorporated in the momentum equation by introducing a volume force $\mathbf{F_b}$ as described by Brackbill et al. [13]. This localized volume force is calculated from the volume fraction data using

$$\mathbf{F_b} = \sigma k(\mathrm{x})\tilde{\mathbf{n}}\frac{\nabla\tilde{\mathrm{F}}(\mathrm{x})}{[\mathrm{F}]}.\frac{\rho(\mathrm{x})}{[\rho]} \tag{3}$$

where k is the curvature of the interface. The interface characteristic parameters of the outward normal vector $\tilde{n}$ and the curvature k are calculated by

$$k = -(\nabla.\hat{\boldsymbol{n}}) = \frac{1}{\tilde{\boldsymbol{n}}}\left[\left(\frac{\tilde{\boldsymbol{n}}}{|\tilde{\boldsymbol{n}}|}\cdot\nabla\right)|\tilde{\boldsymbol{n}}| - (\nabla\cdot\tilde{\boldsymbol{n}})\right] \tag{4}$$

$$\tilde{\boldsymbol{n}} = \left(\tilde{n}_x\tilde{n}_y\right);\ \hat{\boldsymbol{n}} = \frac{\tilde{\boldsymbol{n}}}{|\tilde{\boldsymbol{n}}|} \tag{5}$$

The curvature *k* is given in terms of $\tilde{\boldsymbol{n}}$ and $|\tilde{\boldsymbol{n}}|$ to ensure the main contribution from the finite difference approximation of *k* comes from the centre of the transition region rather than the edges [13].

In VOF method, the motion of the gas-liquid interface is tracked based on the volume fraction function, F. When F is unity, the space is occupied by the liquid phase, when F is zero, the space is occupied by the gas phase and when F is between 0 and 1, the space contains both the gas and liquid phases. The standard advection equation for F is given by

$$\frac{\partial \mathrm{F}}{\partial t} + \nabla.(\mathbf{u}\mathrm{F}) = 0 \tag{6}$$

The volume tracking algorithms are used to capture the interfaces. In this current study, the Piecewise Linear Interface Construction (PLIC) algorithm [14] is adopted to solve Eq. (6) and to reconstruct the interfaces since it has a high accuracy. The mixture properties used in Eq. (2) can be defined by

$$\rho(\mathrm{F}) = \mathrm{F}\rho_l + (1-\mathrm{F})\rho_\mathrm{g} \tag{7}$$

$$\mu(\mathrm{F}) = \mathrm{F}\mu_l + (1-\mathrm{F})\mu_\mathrm{g} \tag{8}$$

The level set method [15, 16] is used with VOF method for the current study is the level set. The level set function $\varphi(r,t)$ is defined by-

$$\varphi(r,t) = \begin{cases} +d & \text{in liquid region} \\ 0 & \text{at interface} \\ -d & \text{in gas region} \end{cases} \tag{9}$$

where *d* is the shortest distance of a point *r* from the interface at time *t*. And the level set equation is given

$$\frac{\partial \varphi}{\partial t} + \mathbf{u}\cdot\nabla\varphi = 0 \tag{10}$$

Therefore, Eq. 2 can be written as

$$\rho(\tilde{\alpha})\left\{\frac{\partial \mathbf{u}}{\partial t} + \nabla.(\mathbf{u}\mathbf{u})\right\} = -\nabla p + \rho(\tilde{\alpha})\mathbf{g} + \nabla.\tau + \sigma k\nabla\tilde{\alpha} \tag{11}$$
$$\tau = [\mu(\tilde{\alpha})\{\nabla\mathbf{u} + (\nabla\mathbf{u})^T\}]$$

where $\tilde{\alpha}$ is the smoothed void fraction and $\sigma\ is$ represents the surface tension. The smoothed void fraction field in the CLSVOF method is defined using a smoothed Heaviside function $H_\varepsilon(\varphi)$, defined as

$$\tilde{\alpha} = H_\varepsilon(\varphi) = \begin{cases} 1 & if\varphi > \varepsilon \\ \frac{1}{2} + \frac{\varphi}{2\varepsilon} + \frac{1}{2\pi}\left[\sin\frac{\pi\varphi}{\varepsilon}\right] & if|\varphi| \le \varepsilon \\ 0 & if\varphi < -\varepsilon \end{cases} \tag{12}$$

Since the density and viscosity of each fluid is constant as the fluid is assumed incompressible, they take two different values as follows

$$\rho(\varphi) = \rho_l H(\varphi) + [1-H(\varphi)]\rho_\mathrm{g} \tag{13}$$
$$\mu(\varphi) = \mu_l H(\varphi) + [1-H(\varphi)]\mu_\mathrm{g} \tag{14}$$

Where H (φ) is the Heaviside function given by

$$H(\varphi) = \begin{cases} 1 & if\varphi > 0 \\ \frac{1}{2} & if\varphi = 0 \\ 0 & if\varphi < 0 \end{cases} \tag{15}$$

In the current study, water is used as the primary phase (liquid) and air is used as secondary phase and the physical properties of the water and the air are shown in Table 1.

Table 1: Physical properties of the liquid and gas in the simulations

Phase	Density (kg/m^3)	Viscosity (Pa.s)	Surface Tension (N/m)
Primary (water)	998.2	1.789e-5	0.0728
Secondary (air)	1.225	0.001	-

2.1 GEOMETRY CONFIGURATION

Two dimensional (2D) domain is used to study the flow of a single bubble in a column. The column basically has a height of 100mm and a width of 50mm to form a rectangular domain. The width of the top wall is reduced to form a trapezoid domain which shown in Figure1.

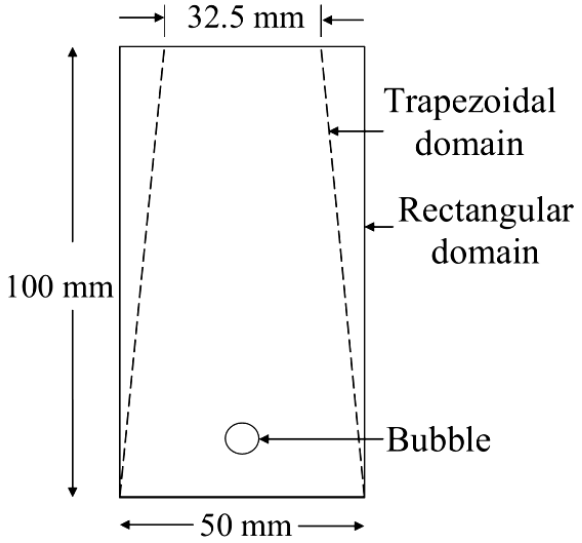

Fig.1: Computational domain of rectangular domain and trapezoidal domain.

At initial stage of a simulation, an air bubble is imposed at the centre and 10 mm height from the bottom of the domain. In this study, three bubble sizes of 3, 4 and 5 mm diameter is studied. The bubble in a quiescent liquid will

rise under the action of the buoyancy force and the bubble rising velocity and its characteristics will be numerically investigated.

2.2 BOUNDERY CONDITION AND NUMERICAL METHODS

The side and bottom walls of the domain are assigned as no slip boundary condition and the top wall as pressure outlet boundary condition. The operating pressure is set to be equal to the ambient pressure, i.e., 101325 Pa and the gravitational force (g) of 9.81 m/s^2 is assigned along –Y direction.

The continuity, momentum and volume of fluid fraction equations were solved using the Ansys-Fluent CFD commercial package, which is based on the finite volume method. The second order upwind scheme was used for the flow equations[17]. The pressure implicit with splitting operators (PISO) algorithm was applied to solve the pressure-velocity coupling[18], which allows a rapid convergence rate without a significant loss of solution stability and accuracy [17]. Pressure was solved using a body force weighted scheme and an implicit body force treatment was applied to improve the solution convergence. The Fluent transient model based on an explicit scheme with a time step of 0.0001s is used which gives a Courant number of 0.25.

2.3 MESH DEPENDENCY TEST

The effect of a mesh size on results was investigated using three types of meshes in the rectangular domain. The dimensions of each cell in these meshes are 0.20mm×0.20mm, 0.25mm×0.25mm, 0.30mm×0.30mm respectively. A structured mesh as shown in Figure 2 is used.

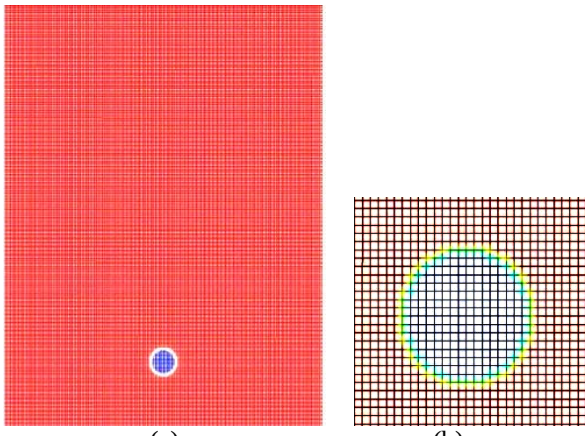

Fig.2: (a) Physical model of single bubble rising process for 0.25mm× 0.25mm mesh size. (b)Zoom view on mesh around the bubble.

The bubble rising distance with the increase of time in second is shown in Figure 3 for the different meshes.

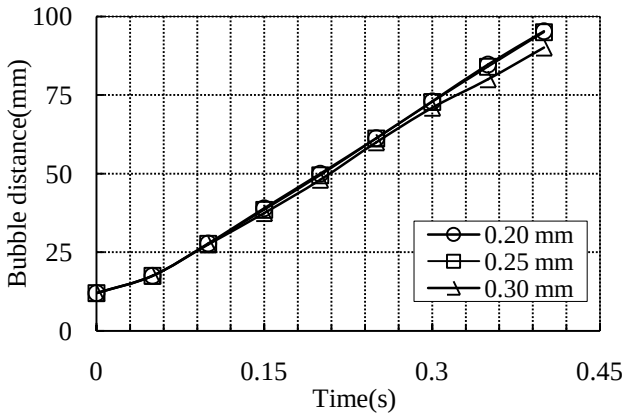

Fig.3: Mesh dependency test for different types of mesh based on 4 mm bubble diameter in rectangular domain.

The results from the mesh with the cell size of 0.20mm×0.20mm are almost the same as that from the cell size of 0.25mm×0.25mm. The results from 0.30mm×0.30mm mesh size slightly differ from that of other meshes especially beyond 0.2s. The results mean that the optimum accuracy can be reached with 0.30mm×0.30mm mesh size. The less dense mesh of 0.25mm×0.25mm is selected based on the accurate results to reduce computational requirements.

3. RESULT AND DISCUSSION

3.1Validation of CFD model

Figure 4a shows the rising velocity of a bubble as a function of time for the rectangular column.

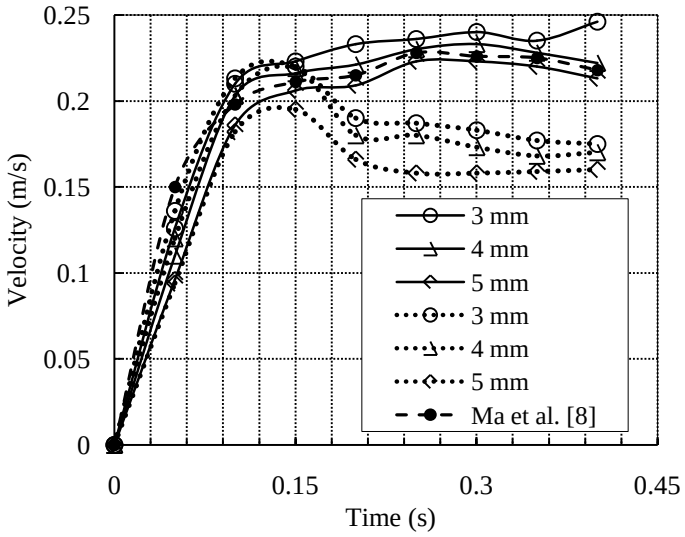

Fig.4a: Bubble rising velocities versus time for different bubble size in the rectangular domain (Solid line) and trapezoidal domain (Dot line). Such data from Ma et al. [8] is also included (Dash line) for 4 mm size of bubble.

The results from our CFD models checked against the numerical and experimental results of D. Ma et al. [8] for 4mm bubble diameter. The results are quite consistent to each other with small differences. In addition, the terminal velocity from our CFD models are also compared with that obtained using Mendelson equation and Clift et al., which is found in Krishna et al.[19] and the equation was given as $V_b=SF\times(2\sigma/\rho_l d_b+gd_b/2)^{1/2}$, where $SF=[1-(d_b/D_t)^2]^{3/2}$. The comparison is shown in Table 2 and the differences are less than 5% for 3-5mm bubble diameters. This suggests that the CFD models are capable of predicting accurate results.

Table 2: Comparisons between simulation results and correlation for different size of bubble [19].

Bubble diameter (mm)	Correlation (m/s)	Simulation (m/s)	Error (%)
3	0.249	0.237	4.81
4	0.233	0.225	3.43
5	0.227	0.216	4.84

3.2 Bubble rising velocity

Figure 4a shows instantaneous velocities of bubbles of 3-5mm diameters in the rectangular domain and trapezoidal domain with respect to time increase. From the initial condition up to 0.1s, the velocities of the bubbles have a steep increase to a peak value of 0.22m/s in the both domains. Following that, the velocities do not change much and remains almost constant around that value in the rectangular domain. However, this is not the case in the trapezoidal domain where the velocity drops from the peak value at 0.15-0.18 seconds before settling near 0.18 m/s velocity.

The difference of velocity of each bubble in the two different columns is shown in Figure 4b in percentage.

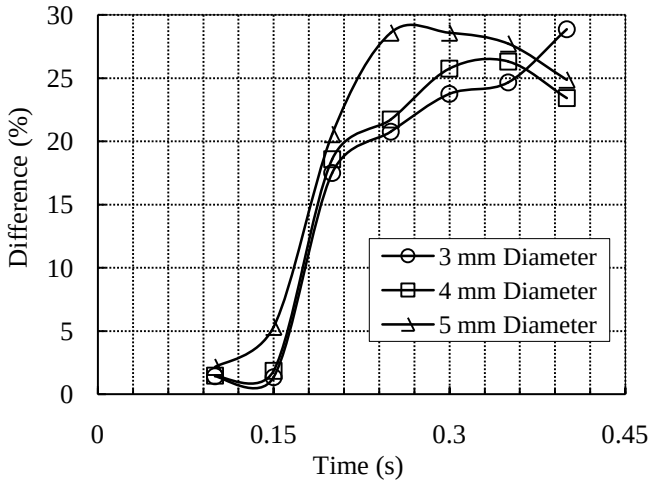

Fig.4b: The difference of the bubble rise velocity between rectangular domain and trapezoidal domain for different size of bubble.

It can be seen that up to 0.15s, the differences are very small. Following that, the difference increases for all bubble sizes. In general, a larger difference occurs for a larger bubble size and vice versa which can be clearly seen at time 0.2-0.35s. For example, the difference is about 23% and 28.5% for 3mm and 5mm bubble diameters, respectively at 0.35s. This results show that trapezoidal column have more effect to a bigger bubble and slows down the rising of the bubble.

Figure5a shows the bubble rising distance with the increase of time up to 0.4s for the three bubble sizes in the two different domains.

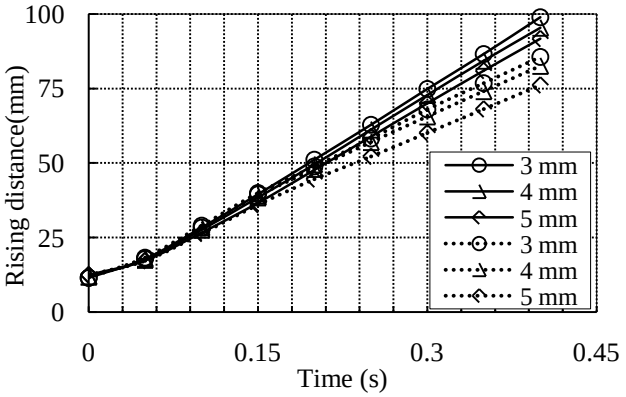

Fig.5a: Bubble rising distance at different times for different bubble size in rectangular domain (solid line) and trapezoidal domain (dot line).

It is observed that up to 0.15s, there is no significant difference in distance for the bubbles moving up from the initial position of 10 mm to 40 mm in the both domains, which is up to 0.15s. Following that, the rising distance is not the same for the bubble in the domains. The distance is the highest for 3mm bubble in the rectangular channel and the lowest for 5mm bubble in the trapezoidal channel.

Figure 5b shows the percentage difference in distance for the bubbles between the two domains.

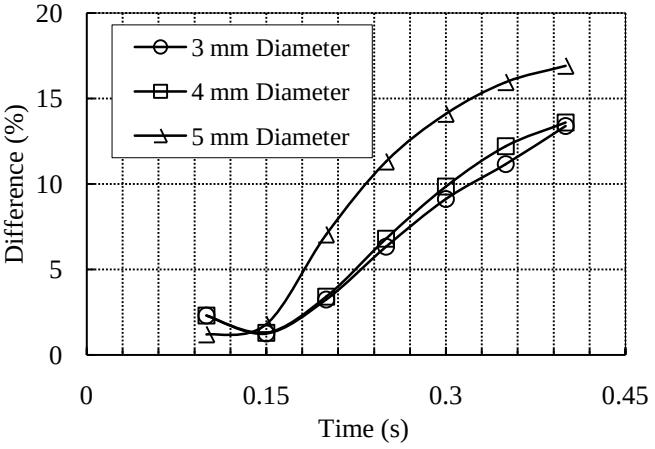

Fig.5b: The difference of the bubble rising distance between rectangular domain and trapezoidal domain for different size of bubble.

It is found that from the figure up to 0.15s, the differences are very small. Following that, the difference increases for all bubble sizes. In general, a larger difference occurs for a larger bubble size and vice versa. For example, the difference is about 13.75% and 17% for 3mm and 5mm bubble diameters, respectively at 0.35s.

3.3 Bubble flow field

In this study, the liquid phase was completely at rest initially due to zero velocity condition. Generally, a single bubble goes to upward due to the buoyancy force and a fluid jet forms at the bottom of the bubble. This jet is pushed the lower surface of the bubble up towards the top surface [21]. The pressure gradient at the lower surface of the bubble is greater than at the top surface of the bubble. Due to this pressure differences, the vortex is forms at the surface with has a rotation and liquid jet that pushes into the bubble from below [21]. The bubble is deformations due to this liquid jet. Generally, the smaller bubbles face less deformation than their larger bubble.

Figure 6a and 6b, represents the vorticity magnitude for 5mm size of bubble in different domain. As seen from Figures, the bubble rose in upward direction and the maximum vortices was located on the side of the bubble in both rectangular and trapezoidal domain. As seen Figure 6b, secondary vortices were formed due to more deformation of bubble that happened by the shape of the domain as well as effect of wall.

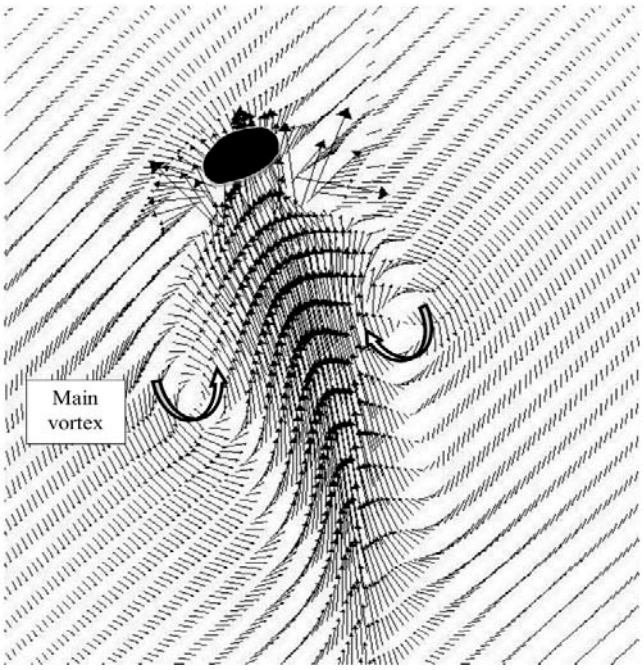

Fig.6a: Velocity vectors of 5mm bubble in rectangular domain at time, t=0.35s.

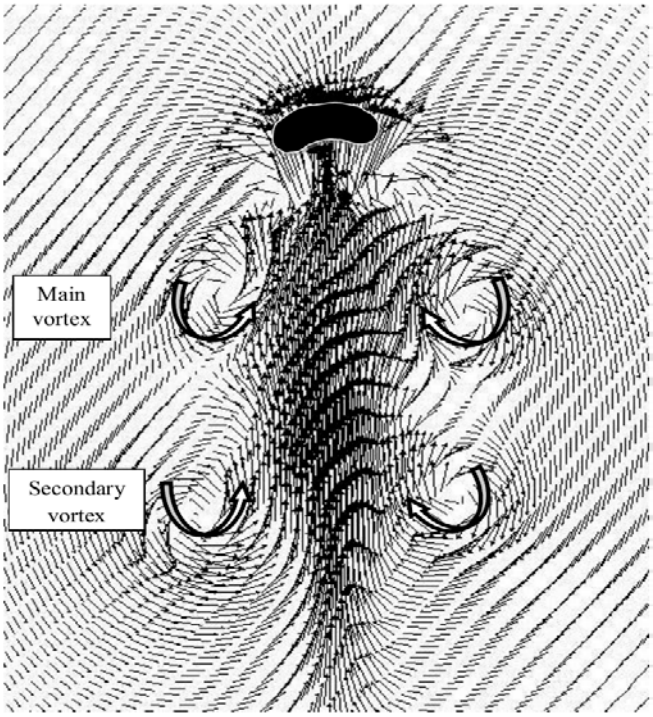

Fig.6b: Velocity vectors of 5mm bubble in trapezoidal domain at time, t=0.35s

4. CONCLUSION

In this paper, the different sizes of bubble in water in two types of domains have been studied numerically using VOF method. The bubble velocity from the CFD models is in good agreement with that from literatures. This study shows bubble velocity is affected by the shape of a column. The bubbles velocity is higher in the rectangular domain and lower in the trapezoidal domain. The effect of wall is apparent in the trapezoidal domain. The velocity distribution around the bubble was also investigated. In the rectangular domain, the bubble deformation is minimum compared to that in the trapezoidal domain.

6. ACKNOWLEDGEMENTS

The authors are grateful to University of Malaya (Project No: UM.C/HIR/MOHE/ENG/13) and University of Malaya Research Grant (UMRG: RG121/11AET) for providing the fund for the research work.

7. REFERENCES

[1] Liu, M.-y. and Z.-d. Hu, *Studies on the Hydrodynamics of Chaotic Bubbling in a Gas-Liquid Bubble Column with a Single Nozzle.*Chemical engineering & technology, 2004. **27**(5): p. 537-547.

[2] Kulkarni, A.A. and J.B. Joshi, *Bubble formation and bubble rise velocity in gas-liquid systems: a review.* Industrial & engineering chemistry research, 2005. **44**(16): p. 5873-5931.

[3] Yang, N., et al., *Multi-scale analysis of gas–liquid interaction and CFD simulation of gas–liquid flow in bubble columns.* Chemical Engineering Science, 2011. **66**(14): p. 3212-3222.

[4] Yang, G., B. Du, and L. Fan, *Bubble formation and dynamics in gas–liquid–solid fluidization—A review.* Chemical Engineering Science, 2007. **62**(1): p. 2-27.

[5] Rabha, S.S. and V.V. Buwa, *Volume-of-fluid (VOF) simulations of rise of single/multiple bubbles in sheared liquids.* Chemical Engineering Science, 2010. **65**(1): p. 527-537.

[6] Chakraborty, I., G. Biswas, and P. Ghoshdastidar, *A coupled level-set and volume-of-fluid method for the buoyant rise of gas bubbles in liquids.* International Journal of Heat and Mass Transfer, 2013. **58**(1): p. 240-259.

[7] Szewc, K., J. Pozorski, and J.-P. Minier, *Simulations of single bubbles rising through viscous liquids using smoothed particle hydrodynamics.* International Journal of Multiphase Flow, 2012.

[8] Ma, D., et al., *Two-dimensional volume of fluid simulation studies on single bubble formation and dynamics in bubble columns.* Chemical Engineering Science, 2012. **72**: p. 61-77.

[9] Buetehorn, S., et al., *CFD simulation of single-and multi-phase flows through submerged membrane units with irregular fiber arrangement.* Journal of Membrane Science, 2011. **384**(1): p. 184-197.

[10] Dai, J., J. Sterling, and A. Nadim. *Numerical simulation of air bubbles rising in water using an axisymmetric VOF method*. in *2 nd International Conference on Computational Methods in Multiphase Flow*. 2003.

[11] Gerlach, D., et al., *Numerical simulation of periodic bubble formation at a submerged orifice with constant gas flow rate.* Chemical engineering science, 2007. **62**(7): p. 2109-2125.

[12] Yan, K. and D. Che, *A coupled model for simulation of the gas–liquid two-phase flow with complex flow patterns.* International Journal of Multiphase Flow, 2010. **36**(4): p. 333-348.

[13] Brackbill, J., D.B. Kothe, and C. Zemach, *A continuum method for modeling surface tension.* Journal of computational physics, 1992. **100**(2): p. 335-354.

[14] Youngs, D., *Time-dependent multi-material flow with large fluid distortion.* Numerical methods for fluid dynamics, 1982. **24**: p. 273-285.

[15] Sussman, M., et al., *An adaptive level set approach for incompressible two-phase flows.* Journal of Computational Physics, 1999. **148**(1): p. 81-124.

[16] Haj-Hariri, H., Q. Shi, and A. Borhan, *Thermocapillary motion of deformable drops at finite Reynolds and Marangoni numbers.* Physics of Fluids, 1997. **9**: p. 845.

[17] Akhtar, A., *CFD Simulations for Continuous Flow of Bubbles through Gas-Liquid Columns: Application of VOF Method.* Chemical Product and Process Modeling, 2007. **2**(1): p. 1-19.

[18] Issa, R.I., *Solution of the implicitly discretised fluid flow equations by operator-splitting*. Journal of Computational physics, 1986. **62**(1): p. 40-65.

[19] Krishna, R., et al., *Wall effects on the rise of single gas bubbles in liquids.* International communications in heat and mass transfer, 1999. **26**(6): p. 781-790.

[20] Fluent, A., 2009. 12.0 User's Guide. ANSYS.

[21] Karthik, Quan and Portonovo, *Numerical study of wall effects on buoyant gas-bubble rise in a liquid-filled finite cylinder.* Physical Review E, 2007 **76**:p.036308

8. NOMENCLATURE

Symbol	Meaning	Unit
G	gravitational acceleration	(m/s^2)
H	Heaviside function	
p	Pressure	(Pa)
μ	viscosity of fluid	(Pa s)
ρ_l	density of fluid	(kg/m^3)
σ	surface tension coefficient	(N/m)
V_b	Terminal velocity	(m/s)
d_b	bubble diameter	(mm)
D_t	Column diameter	(mm)
SF	Scale factor	[-]